Advances in Science and Technology Research Journal, 2025, 19(12), 1–16 https://doi.org/10.12913/22998624/209071 ISSN 2299-8624, License CC-BY 4.0

# Accepted: 2025.10.01 Published: 2025.11.01

Received: 2025.07.07

# Extracting selected tilted fibre Bragg gratings spectrum features

Marta Dziuba-Kozieł<sup>1</sup>, Grzegorz Kozieł<sup>1\*</sup>

- <sup>1</sup> Faculty of Electrical Engineering and Computer Science, Lublin University of Technology, Nadbystrzycka 38A, 20-618 Lublin, Poland
- \* Corresponding author's e-mail: g.koziel@pollub.pl

#### **ABSTRACT**

Tilted fibre Bragg gratings (TFBG) are used as sensors in the measurement of many physical and chemical quantities. Measurement is performed indirectly by analysing the power of light transmitted at a specific wavelength or in a selected range of light wavelengths. The wavelengths to be used are chosen arbitrarily by the researcher. However, a change of parameters of the TFBG grating requires reselection of the wavelengths to be used in the measurement. Due to the fact that the TFBG spectrum most often shows the most significant sensitivity to changes in the measured parameters in the cladding mode range or a shift of the Bragg resonance, these are most often used in measurements. The need for human selection of the wavelength range to use was the motivation to undertake research into a method for automatic feature extraction of the TFBG spectrum. The method is designed to enable the identification of the cladding mode minima, the range of wavelengths at which they occur, and the wavelength at which the Bragg resonance occurs. In addition, the heights of the cladding mode minima and the Bragg mode were calculated. The developed algorithm detects key features of TFBG transmission spectra for both P and S polarisation. It automatically identifies the cladding mode range, including their minima and maxima. Furthermore, it allows the determination of the position and height of the Bragg mode for TFBGs with tilt angles up to 6 degrees. The present solution is a pioneering work providing a basis for automating the selection of wavelength ranges or spectrum features for use in TFBG-based sensors.

Keywords: tilted fibre Bragg gratings, feature, fibre, light, spectrum, optic.

#### INTRODUCTION

Tilted fibre Bragg gratings (TFBGs) are used as sensors to measure many physical and chemical quantities [1, 2]. However, the measurement effect obtained often depends on selecting appropriate parameters of the fibre and TFBG structure [3, 4]. It is also important to use appropriate fibre core material doping [5]. The spectral response depends on the Bragg structure's tilt angle, their spacing, and the amplitude of refractive index changes in the core [6, 7]. Also, the cut-off wavelength shift caused by a change in the surroundings2 refractive index (SRI) depends on the tilt angle [8]. The spectral response of TFBG can be analysed in its entirety, but in this case, the wavelength range in which the light spectrum is measured is adjusted. This type of solution is used to

measure the bending radius or twist of an optical fibre [9, 10]. An analogous situation occurs when measuring the angle of rotation of the plane of polarisation of light [11, 12]. Also, pH and pressure measurements require selecting the correct wavelength range of light [13, 14]. In the process of detecting mercury ions, the shift of the selected minimum of the cladding modes is studied [15]. In the SRI measurements, the shift in cutoff wavelength that occurs in the cladding mode region is analysed [16, 17]. A problem found in many works is switching between spectral peaks caused by spectrum shift when SRI changes [18, 19]. TFBGs are also used to detect and measure concentrations of various substances [20, 21]. This is possible by coating them with a thin layer of a substance that changes its SRI under the influence of absorption of the molecules of the

detected substance [22, 23]. Also important is the fact that the sensitivity of the sensor can depend on the choice of the cladding mode or the wavelength range of the light being analysed [24]. As shown in [25], various modes of light propagating by TFBGs show varying levels of sensitivity to temperature changes. It was demonstrated in [1] that different portions of the light spectrum exhibit sensitivity to different external factors. In sensors that allow simultaneous measurement of multiple parameters, it is necessary to identify multiple features of the TFBG spectrum [26, 27].

In all cases presented, selected wavelength ranges or specific spectral features are analysed, such as the location of minima of selected modes or distances between them. In the case of the described solutions, the researcher arbitrarily selects features or wavelengths to be used on the basis of spectrum analysis. The use of TFBGs having different parameters forces a re-analysis of the spectrum and selection of the range of wavelengths of light or features to use. This process could be automated through the use of spectrum analysis algorithms to identify its key features. Existing methods for the analysis of the transmission spectrum of TFBGs focus on the extraction of single spectral features dedicated to specific sensors. This motivated the development of a method allowing the identification of key features of the transmission spectrum of TFBGs. The main goal of the paper is to create a method for analysing a spectrum of light propagating through the TFBG and extracting its features, such as the position of the Bragg mode, the wavelength range of the cladding mode area, as well as the position of the cladding mode minima and their heights.

The rest of the paper is organised as follows: the related works section analyses existing signal processing solutions used to analyse the spectral response of TFBGs. The Materials and Methods section discusses the basics of Bragg gratings, presents the measurement setup and discusses the proposed method for extracting selected features of the TFBG spectrum. In the Discussion and results section, the results obtained are presented and discussed. A summary and conclusions of the work carried out are included in the Conclusions section.

#### **Related works**

Signal processing uses many methods. Various types of transforms, filtering, machine learning, and deep learning, which find application in

many fields [28, 29]. Some of them can be successfully used to process the light spectrum, but to obtain satisfactory results it is necessary to properly select features to examine [30].

The authors of [31] have developed a method for determining the plasmon resonance wavelength based on the analysis of the TFBG transmission spectrum. They do this by determining the superposition of a set of maxima or minima near the plasmon resonance wavelength. The light spectrum is pre-filtered to remove high-frequency components. Filtering is done by calculating the light spectrum's Fast Fourier Transform (FFT) and removing the coefficients representing the high-frequency components. The spectrum is then aligned with the horizontal axis and lowpass filtered again using the FFT. The minima and maxima of the filtered signal are then determined by identifying the wavelengths of light for which the derivative of the signal changes sign, after which the heights of all peaks are calculated and the position of the peak closest to the spectral constriction is initially determined. Due to the low precision of the method, the authors propose three additional methods to determine the position of the spectral constriction precisely. Two of these involve fitting functions defined by the authors to maxima adjacent to the pre-determined spectral constriction. The minimum of the function determines the correct wavelength of the spectral constriction. The third method is also based on a search for the extremum of a function. It incorporates two functions – one is fitted to the maxima and the other to the minima of the filtered signal.

Despite the development of algorithms for determining the position of the spectral constriction, the proposed method is not fully autonomous – it requires a significant number of parameters whose values depend on the TFBG parameters.

In [32], a method for determining the cutoff position in the light spectrum is presented. The light spectrum was pre-filtered and aligned according to the method presented in [31]. The upper and lower envelopes of the spectrum were then determined by approximating the maxima and minima with the smooth curves proposed by the authors. Their inflection points were then determined, which were used to determine the wavelength cut-off position.

The other approach to SRI measurement was proposed in [33]. Gabor filters were used to filter and process TFBG spectrum. At first spectrum was lowpass filtered and aligned. Then envelope

shifts and envelope derivatives were used to determine SRI. A linear relationship between the shift of the maximum of the first derivative and the change in SRI was identified.

The envelope of the low-pass filtered light spectrum was also used in [34] to evaluate changes in the light spectrum caused by a change in the angle of polarisation plane rotation of the light reaching the cascade of two TFBGs. However, the authors limited themselves to only analysing the field between the lower and upper envelopes of the signal.

In [11, 12], a transformation of the spectrum of light propagating through the TFBG using wavelet and Fourier transforms is applied. In both cases, the change in the value of selected transform coefficients or groups of transform coefficients is analysed to measure the angle of rotation of the plane of polarisation of the light.

#### MATERIALS AND METHODS

#### Construction and working principle of TFBGs

A tilted Bragg grating is a structure created in the core of an optical fibre. By irradiating the fibre, the refractive index of selected areas of the optical fibre is modified. In this way, planes of altered refractive index are created in the core. In the case of fibre Bragg gratings (FBGs), the planes produced coincide with the axis normal to the fibre. In the case of TFBGs, they are positioned at the non-zero angle to the axis normal to the fibre and this angle is called the tilt angle of the structure  $(\Theta)$ . The presence of a TFBG in the fibre core causes some of the light propagating through to be reflected to the fibre's cladding, causing a series of minima in

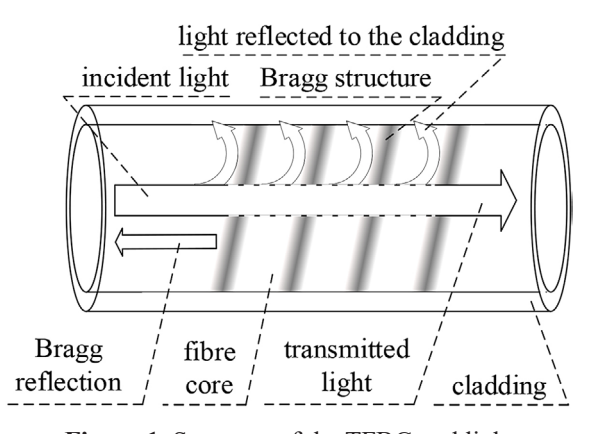


**Figure 1.** Structure of the TFBG and light propagation within the TFBG

the transmission spectrum called cladding modes. Part of the light is reflected along the fibre axis creating an additional minimum in the transmission spectrum called a Bragg mode. The remainder of the light is transmitted through the fibre. The wavelengths at which the individual minima occur depend on the  $\Theta$  and the distance between the Bragg structures [35]. A schema of the TFBG structure and the propagation of light within the TFBG is shown in Figure 1.

### Interrogation setup

The light spectra used in this work were captured using the system shown in Figure 2. The light emitted by the superluminescent diode (SLED) is propagated through a polariser and a half-wave plate, allowing the angle of rotation of the light polarisation plane to be controlled. The light is then divided by a 50:50 splitter into two beams, one of which is directed to the TFBG and the optical spectrum analyser (OSA) attached to it, while the other to an additional spectrum analyser. In this way, the spectrum of light propagating through the TFBG and the spectrum of the light source can be recorded.

The system in question used a Thorlabs S5F-C1550S-A2 light source (SLD), Thorlabs CFP2-1550A collimators, an electronically controlled half-wave plate Thorlabs WPHSM05-1550, and Yokogawa AQ6730D spectrum analysers.

The present study investigated the spectral responses of 10 TFBGs with tilt angles  $\Theta \in \{1,2,...,10\}$ . The studied TFBGs were fabricated according to the phase mask method using an excimer laser. For each grating, spectra for P and S polarisation were recorded. Wavelengths of light from 1400 nm to 1660 nm were recorded with the OSA sensitivity set to MID with a resolution of 0.0052 nm.

# Transmission spectrum of a TFBG and its components

The light propagating through the TFBG is modified due to the reflection of parts of light of different wavelengths. The reflected light components do not propagate through the TFBG, resulting in minima in the transmission spectrum of the light. Figure 3 shows the spectra of light propagating through the TFBG with  $\Theta$ =4° and the light source that was used in this study. In the TFBG spectrum, the Bragg resonance and the cladding

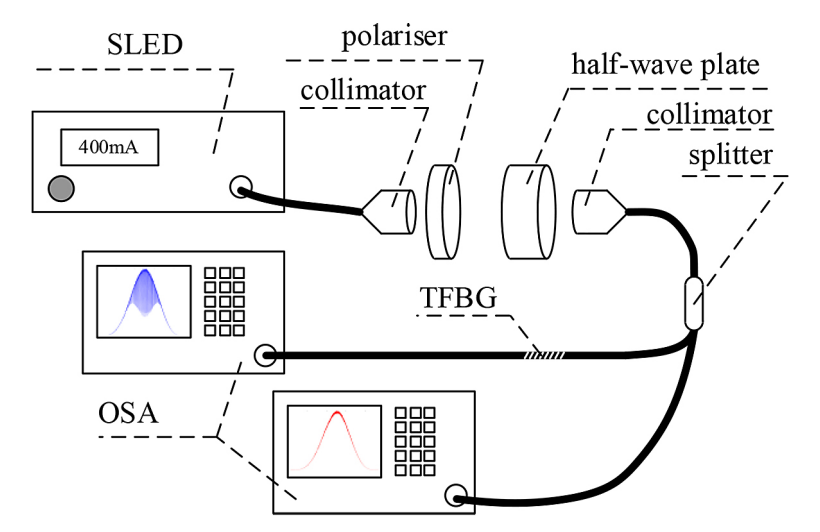


Figure 2. Interrogation setup

mode region are marked. From the point of view of sensor design, these are the most essential parts of the spectrum. The cladding mode region shows the most significant sensitivity to changes in measured physical and chemical parameters[10].

The TFBG spectrum shown in Figure 3 is distorted. The TFBG reflects wavelengths of light with varying efficiency. The power of the reflected light is proportional to the power of the light generated by the light source at a given wavelength. SLED light sources used in laser technology generate light of different powers at different wavelengths (Figure 3). Therefore, the transmission spectrum of the TFBG depends on the spectrum of the light source. Researchers usually divide the transmission spectrum of TFBGs by the spectrum of light fed into the TFBG. This reduces the light source's uneven power impact across wavelengths. However, the problem is that the spectra are noisy due to both the noise

generated by the light source and the noise of the measurement system, which can introduce wavelength shifts of the minima. Therefore, this paper proposes dividing the TFBG spectrum by the approximation of the light source spectrum obtained by regressing the SLED spectrum with an 8th-degree polynomial. A plot of the calculated approximation is included in Figure 3. The approximation used reproduces the SLED light spectrum well in its central part. However, there are distortions near the ends of the approximated range. For this reason, measurements were made in a more extensive range of wavelengths than necessary from the point of view of the present research, and the extreme parts of the spectrum and their approximation were omitted.

In the remainder of this article, the TFBG spectra divided by the light source spectrum approximation will be used (Figure 4). For the purposes of this article, light spectra for each

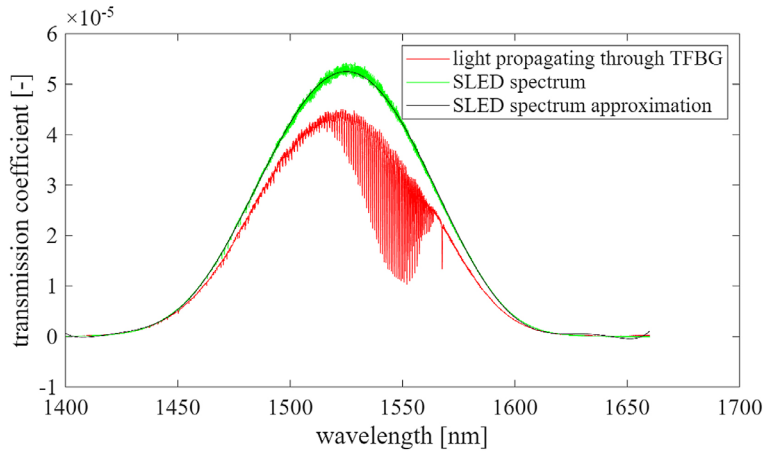


Figure 3. SLED and TFBG light spectra

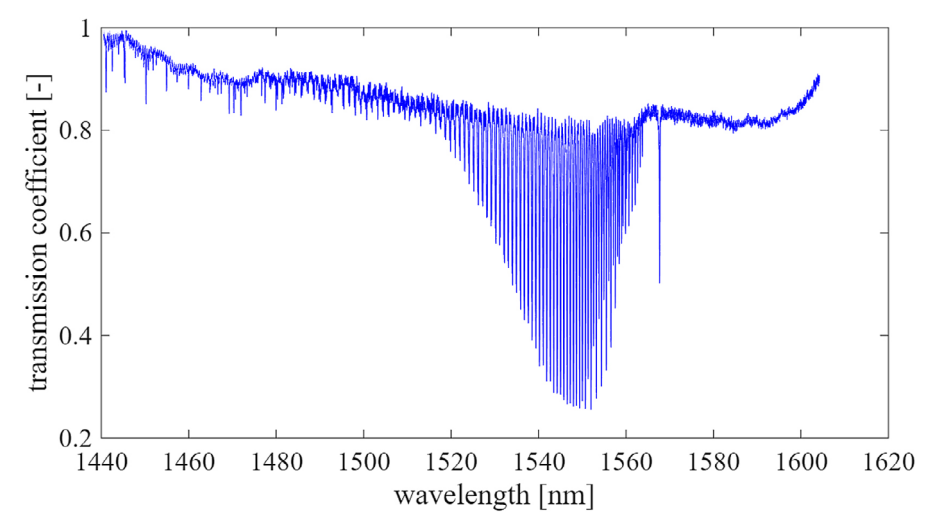


Figure 4. TFBG spectrum divided by the approximation of SLED spectrum

examined TFBG were measured for S and P polarisation at a resolution of 0.005 nm with the OSA sensitivity set to medium.

# A method for the coarse identification of minima in a spectrum

Due to the noisy nature of the light spectra, direct detection of minima is not possible. There are many local minima in the spectra due to the presence of interference. For this reason, a coarse identification of the wavelengths of light at which the minima occur was first made according to the algorithm presented in Figure 5. All samples, being a minimum in the interval R = [x - 0.1 nm, x + 0.1 nm], where x is the wavelength corresponding to the analysed minimum, were searched for. The size of the R interval results from the measured distance between consecutive cladding mode minima. For TFBGs with a tilt angle between  $1^{\circ}$  and  $10^{\circ}$ , it

ranges from 0.15 nm to 1.7 nm. It is worth noting that the distance between cladding mode minima varies in wavelength and is also affected by the tilt angle of the TFBG. In Figure 5, this range was given as a number of samples resulting from the sampling resolution used. Each of the identified minima was verified by checking if the samples' values on either side of the identified minimum are ascending sequences. Samples in these sequences were numbered so that the smallest indexes had samples adjacent to the local minimum analysed, and the largest indexes had samples furthest away. Due to possible noise, non-monotonic sequences meeting the constraint defined by Equation 1 were also allowed:

$$w_{i+1} > w_i + D \tag{1}$$

where:  $w_{i+1}$  is the value of the i+1-th sample of the string,  $w_i$  is the value of the i-th sample of the string, and D is the accepted value difference defined by equation 2:

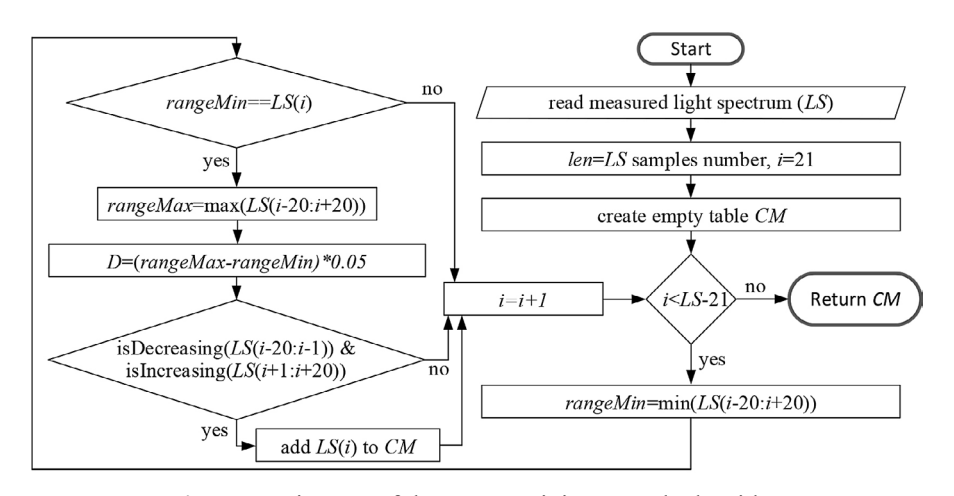


Figure 5. Diagram of the coarse minima search algorithm

$$D = (\text{Max}(R) - \text{Min}(R)) \times 0.05 \tag{2}$$

where: Max(*R*) and Min(*R*) denote the largest and smallest sample value, respectively, in the interval *R*.

All samples satisfying the above conditions are stored in the coarse minima (*CM*) set. The scheme of the algorithm verifying if a sequence of samples is decreasing is presented in Figure 6.

# Determining the width of the search window

Searching for the minima of individual modes in the noisy TFBG spectrum requires estimating the largest distance between the minima of the cladding mode range. For this purpose, the distances between consecutive minima from the CM set are calculated on the base of coarse minima search result performed with algorithm presented in Figure 5. Experimentally, it has been found that up to 10% of the largest distances contain erroneous values due to the omission of some minima in the spectrum. For this reason, these distances are discarded. To minimise the impact of significant differences that may exist in the set of calculated distances, the average of the distances between the 80th and 90th percentiles of the distances arising from the coarse minima search algorithm is taken as the initial search window size  $(WS_{init})$ .

## Determining the list of spectrum minima

The minima search method uses a search window, which is a separate sequence of consecutive samples of the light spectrum. The search window has a specified size (WS), which is defined, on the base of ocarse minima search result, as the number of samples of the spectrum, set to the value  $WS_{init}$  at the start of the search for minima. A window of this size is used to search for the first

six minima. As the distances between the minima of the cladding modes decrease with increasing wavelength, the window size is modified during the search process. Its size is set to the average of the distances between the last six minima, with a window no smaller than 0.15 nm. A 0.15 nm window is used when the calculated window size is smaller.

The search begins by setting the window at the start of the TFBG spectrum and identifying the sample  $(P_{min})$  with the smallest value  $(W_{min})$ within the window. If the sample is close to the window edge, it must be verified as a true local minimum. This is done by verifying that the sample is the minimum in a window centred on it with a size of 0.8WS. If it meets this condition, it is added to the list of minima found (ML), if it has not already been placed there. If the verified minimum does not meet the condition, its distance from the last minimum in the ML list is calculated. If this distance is greater than 2WS, then it is verified whether the analysed sample is a minimum in a 0.1 nm interval centred on it. If so, it is added to the ML list. Verifying this additional condition allows the identification of local minima at the boundaries of the spectrum, which may have an increasing or decreasing trend (see Figure 4) due to imperfections in fitting the spectrum approximation of the light source.

After verifying the minimum found in the search window, the size of the search window is modified, and the window is shifted to the right by 0.1 WS. Finally, minima less than 3% of the height of the largest minimum of the cladding modes are removed from the list of minima. This helps eliminate false minima outside the cladding mode region. The diagram of the minima search algorithm is presented in Figure 7. To simplify the diagram, it omits the protections against exceeding the range of arrays.

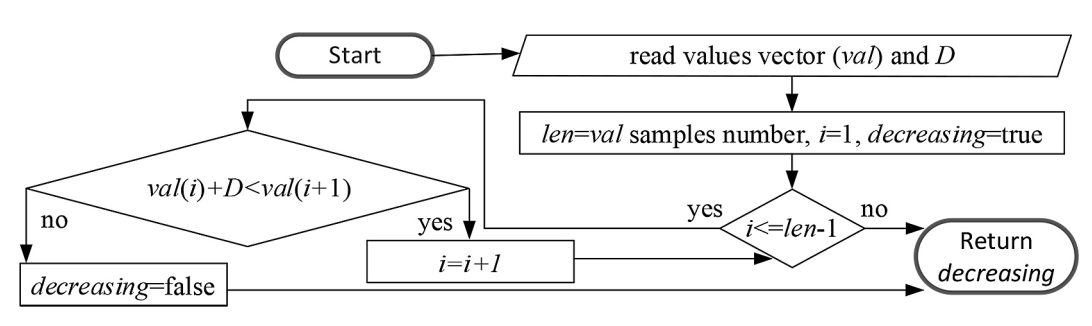


Figure 6. Diagram of the decreasing function

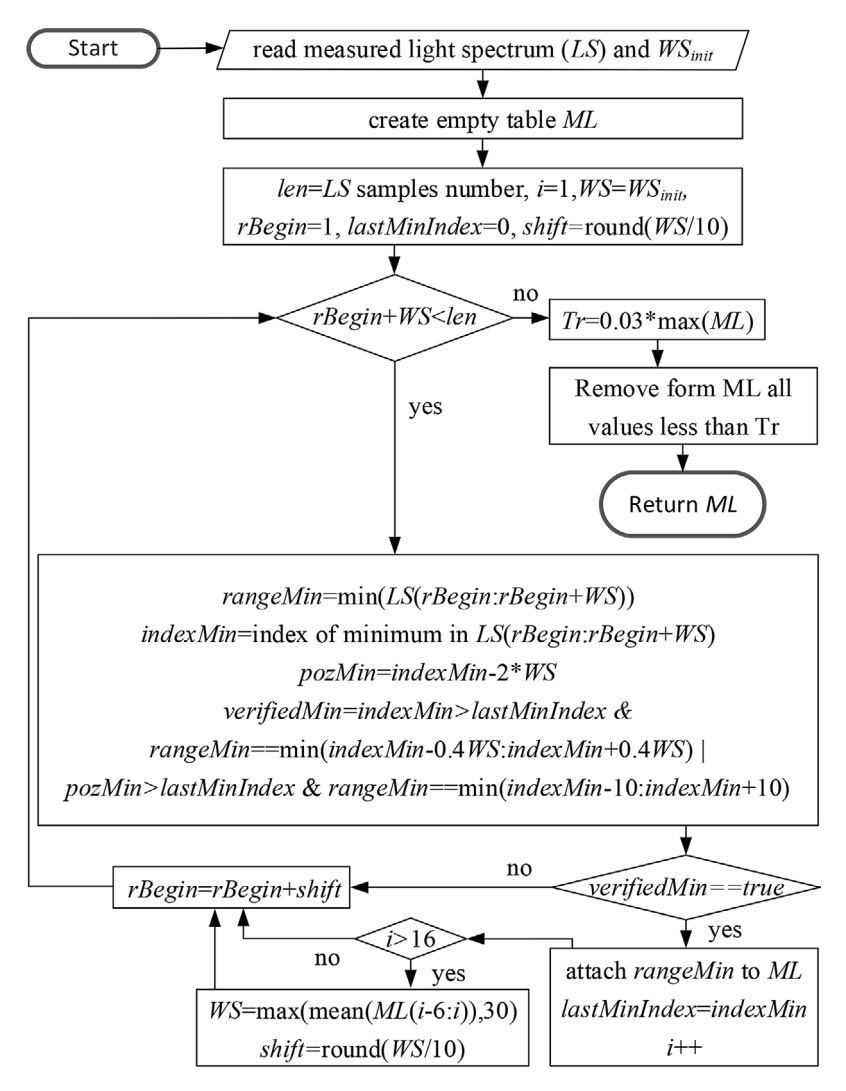


Figure 7. Diagram of the minima search algorithm

#### Calculating the mode height

The mode height (MH) is defined as the difference between the largest and smallest value of the transmission coefficient occurring in the mode wavelength range. The smallest value occurs at the mode's minimum and is easy to identify. It is difficult to identify the largest mode's value. Firstly, the result of dividing the TFBG spectrum by the light source spectrum is distorted, resulting in different values between the maxima occurring on the two sides of the minimum, as can be observed in Figure 8. Secondly, it is difficult to determine the boundaries of individual modes unambiguously. To address the issues identified, the maximum value was determined by finding the highest transmission coefficient on the left  $(max_i)$ and right  $(max_{D})$  sides of the mode's minimum. The mode's maximum value was then calculated as the average of these two values:

$$max_{M} = (max_{I} + max_{R})/2 \tag{3}$$

To avoid determining a mode's boundaries, each of the maxima  $(max_L, max_P)$  was sought in the interval between the minimum of the analysed mode and the nearest identified neighbouring mode's minimum. Figure 8 shows a spectrum fragment where the minimum of the analysed mode is marked with a black asterisk and the minima of neighbouring modes are marked with blue asterisks. The red colour indicates the range in which  $max_L$  was searched, and the green colour the range where  $max_P$  was searched. The mode's height was calculated according to the formula:

$$MH = max_{M} - min_{M}, \tag{4}$$

where:  $min_M$  is the value of the transmission coefficient at the minimum of the analysed mode.

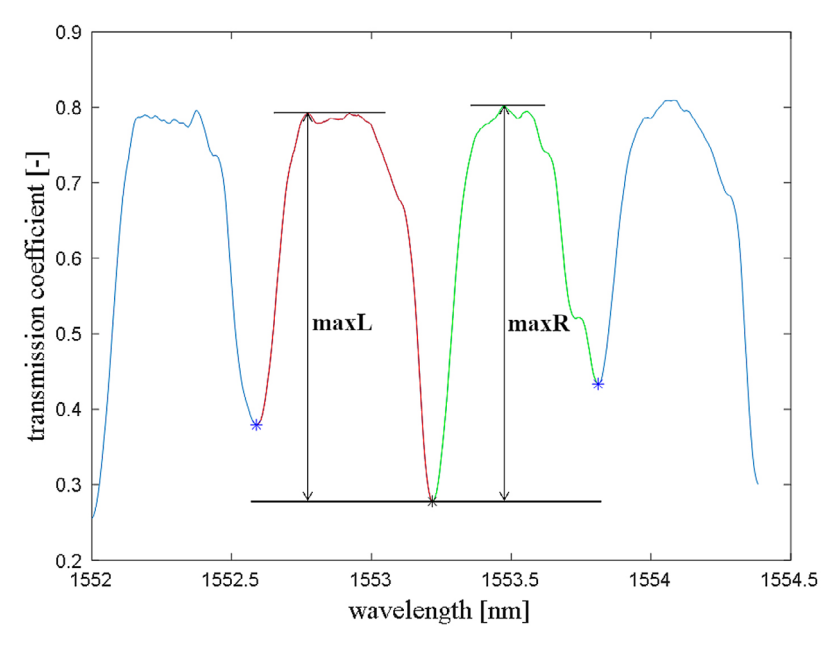


Figure 8. Mode height calculation

#### Determining the largest cladding mode

Depending on the tilt angle of the Bragg structures, the largest cladding mode, ghost or Bragg mode may have the greatest height. To identify the occurrence of any of these modes, it is sufficient to analyse the three largest minima of the spectrum. However, measurement interference can cause additional minima to appear in the actual measurement spectrum, which the proposed algorithm will detect. An example of

such interference is shown in Figure 9, where the Bragg mode can be seen to have been identified as two independent minima in the fragment of the spectrum shown. In the most unfavourable scenario, the ghost and Bragg modes are larger than the largest sheath mode and, due to the interference, each has been classified as two independent minima. In this situation, the biggest cladding mode will be the fifth largest maximum of the spectrum. To account for the occurrence of the present scenario, the five largest minima of

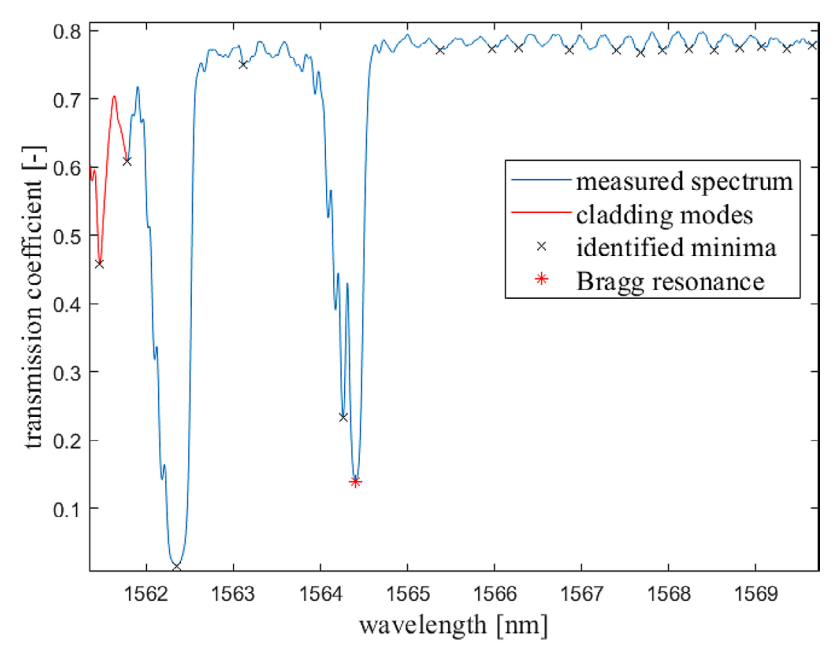


Figure 9. Spectrum fragment containing measurement artefacts

the TFBG spectrum, hereafter denoted as *Max-5Modes*, are analysed in the search for the largest cladding mode. They are analysed sequentially, starting from the minimum occurring at the shortest wavelength of light. If a minimum is found that meets the conditions set for the largest cladding mode, the search is terminated.

The distinction between the largest cladding mode from the ghost and the Bragg modes can be made by analysing their neighbourhood. The Bragg mode is adjacent to modes of relatively small height. Exceptions can be made for spectra of TFBGs having small  $\Theta$  angles, where modes of considerable height, in particular ghost type, can be found to the left of the Bragg mode. In the case of the largest cladding mode, modes of similar magnitude occur on both sides of it. Therefore, the 20 minima with the most significant height were identified in the whole spectrum, and the height of the lowest of these  $(H_{20})$ was determined. Then, for the minima from the Max5Modes set, an evaluation was performed by verifying that the minimum being evaluated is the largest among the six preceding and six following identified minima of the spectrum, and that there are at least six minima among 12 compared neighbouring minima meeting the condition:

$$H_i \ge H_{20} \tag{5}$$

where:  $H_i$  is the height of the minimum.

The first minimum from the set of *Max-5Modes* satisfying the above conditions is the highest cladding mode minimum. In the following, it will be denoted by *MaxCMode*, and its height will be denoted by the symbol *HMCM*.

#### Filtering the minima list

The method of determining the list of spectrum minima detects some other minima, in addition to the mode minima, generally with much smaller values, which are local signal minima. Their presence in the list of detected TFBG spectrum minima is undesirable, as it may interfere with the cladding mode range identification method. For this reason, a method for filtering the list of found spectral minima is proposed. In this method, the height of each identified minima  $(H_i)$  is compared with the heights of four neighbouring minima – the two nearest to the shorter wave side and the two nearest to the longer wave side. If the height of any of the neighbouring minima is less

than  $0.5H_i$ , then that minimum is removed from the list of identified minima. The method works well in the lower wavelength range of the cladding mode region. It may produce undesired effects in the vicinity of ghost and Bragg modes in the case of TFBGs with small values of  $\Theta$ . Because of this, the method is applied only for minima located to the left of the largest cladding mode minimum.

#### Determining the cladding mode range

Calculating the wavelengths corresponding to each mode [35] allows for precisely identifying the cladding modes and their range. However, this is not possible in the case under consideration because the only data we have is the spectrum of light propagating through the TFBG.

In practical applications, a specific cladding mode or a range of the light spectrum in which the cladding modes have significant heights is selected. Therefore, this paper proposes a simplified method for determining the cladding mode wavelength range. It is defined as the range of modes adjacent to the largest cladding mode whose height is a certain percentage (*PM*) of the *HMCM* height.

In the case of TFBGs with small angles  $\Theta$ , the ghost mode may be adjacent to cladding modes with significant heights. For this reason, in searching for the right boundary of the cladding mode region, it is also checked whether the height of the analysed minimum does not exceed the height of the highest of the four preceding minima. If this is the case, this minimum is treated as a ghost mode outside the cladding mode area.

#### Identifying the Bragg mode

The Bragg mode can be located directly to the right of the cladding mode region, or it can be shifted further towards the longer wavelengths of light. For TFBGs having a small  $\Theta$ , it is much larger than the adjacent minima. As  $\Theta$  increases, the Bragg mode decreases. In the present work, the detection of the Bragg mode is realised by analysing the height differences of the neighbouring minima occurring on the right side of the identified cladding mode region, calculated according to the formula:

$$D_{i} = |H_{i} - H_{i-1}| \tag{6}$$

where: i is the index of the minimum,  $H_i$  is the height of the i-th minimum,  $H_{i-1}$  is the

height of the i-1st minimum, and  $D_i$  is the height difference between the i-th minimum and the one preceding it.

The right boundary of the cladding modes area is determined using the algorithm outlined in the previous section, with PM=20%. This PM value was chosen to include as many minima of the cladding modes as possible within the detected area. Additionally, the use of PM=20% ensures that the algorithm does not include minima outside the cladding modes. Thanks to this approach, reliable detection of the right boundary of the cladding modes area is achievable.

A subset  $D_{max}$  containing the four largest differences is created from the set of  $D_i$  differences. Then the indices of the minima, which correspond to the values from the set  $D_{max}$ , are verified. If these are consecutive indices, it means that a minimum has been identified that differs significantly in value from its neighbours. Such minima are verified by checking whether they satisfy the condition:

$$H_i > 2 \times \text{Med} (\{H_{i-3}, H_{i-2}, H_{i-1}, H_{i+1}, H_{i+2}, H_{i+3}\})$$
 (7)

where: *i* is the index of the Bragg minimum and Med denotes the median of the set of values. If two minima satisfy the condition defined by Equation 7, then the Bragg resonance is the minimum at the larger wavelength.

If a Bragg resonance could not be found, then the minima between which the value differences recorded in the  $D_{\max}$  set were identified are subjected to analogous verification. If more than one minimum is successfully verified, it is assumed that the Bragg resonance is the minimum occurring at the biggest wavelength. If none of the minima passes verification, it means that the proposed method cannot identify the Bragg resonance.

### **RESULTS AND DISCUSSION**

#### Minima identification

The developed algorithm allows the identification of TFBG spectrum minima measured at S or P polarisation. The algorithm's task is to identify the minima of the cladding mode range and the Bragg mode, as these are the most commonly used in measurements due to their high sensitivity to changes in measured parameters. All steps of the algorithm presented in the Materials and

Methods section are obligatory and have to be applied to obtain the correct result.

The identification of minima involves several steps. In addition to mode minima, coarse minima identification returns many additional minima, which are local minima in the light spectrum. The results obtained make estimating the greatest distance between cladding modes possible. On this basis, a search for spectrum minima is possible. The search process uses the calculated distance between minima, based on which the width of the search interval is determined. The design of the proposed algorithm guarantees the detection of all cladding mode minima. However, the presence of noise in the TFBG spectrum prevents the effective rejection of other local minima of the spectrum. For this reason, many of the local minima, often resulting from spectrum noise, are placed in the set of identified minima. Only minima with a small value identified inside the cladding mode region are a problem. As these minima are significantly lower than the cladding mode minima, it is possible to identify and remove them from the set of identified minima using the proposed filtering method for the list of minima. Figure 10 shows a fragment of the TFBG spectrum with the minima identified in the successive steps of creating the list of minima of the TFBG spectrum. It can be seen that the minima identification algorithm correctly identified all the cladding mode minima in the central part of this area. In the left part of the cladding mode region corresponding to shorter wavelength light waves, many additional local minima of small height were identified (see Figure 10). These minima were successfully detected and removed from the set of minima by the minima list filtering algorithm. The algorithm works correctly only if cladding mode minima are at least twice as high as noise-induced minima. It is also impossible to apply the filtering algorithm to the right part of the cladding mode spectrum, because some cladding mode minima can be removed from the minima list if there is a ghost mode immediately behind them, being at least twice as high as the adjacent cladding mode minima.

The effectiveness of the method for detecting minima and determining the range of cladding modes, as well as detecting the largest cladding mode minima, was verified. It was done by using the developed method to identify the aforementioned spectral features. The test was performed

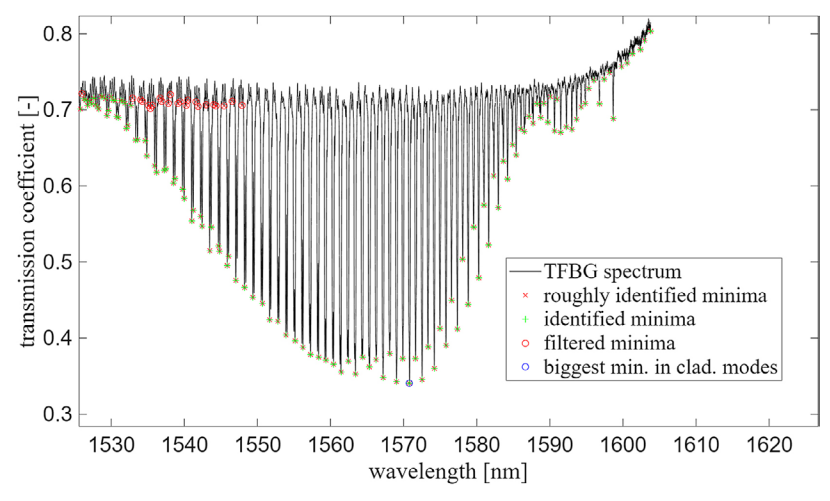


Figure 10. Minima identified in the spectrum

**Table 1.** Features extraction result for *PM*=10%

Θ	Correctly identified cladding mode minima	Additional minima detected	Not detected minima	Correctly identified cladding mode range
1	97.3%	5.4%	2.7%	yes
2	98.6%	1.4%	1.4%	yes
3	98.9%	1.9%	1.1%	yes
4	100.0%	1.6%	0.0%	yes
5	100.0%	0.0%	0.0%	yes
6	100.0%	0.0%	0.0%	yes
7	100.0%	0.0%	0.0%	yes
8	98.5%	1.5%	1.5%	yes
9	100.0%	5.6%	0.0%	yes
10	100.0%	0.0%	0.0%	out of range

**Table 2.** Features extraction result for *PM*=20%

Θ	Correctly identified cladding mode minima	Additional minima detected	Not detected minima	Correctly identified cladding mode range
1	97.0%	0.0%	3.0%	yes
2	98.6%	1.4%	1.4%	yes
3	100.0%	0.0%	0.0%	yes
4	100.0%	0.0%	0.0%	yes
5	100.0%	0.0%	0.0%	yes
6	100.0%	0.0%	0.0%	yes
7	100.0%	0.0%	0.0%	yes
8	100.0%	0.0%	0.0%	yes
9	100.0%	0.0%	0.0%	yes
10	100.0%	0.0%	0.0%	yes

for three *PM* values: 10%, 20% and 30%. The results obtained are presented in Tables 1–3.

The proposed algorithm reliably detects minima in the TFBG spectrum. Setting the PM > 30% allows error-free detection of minima

of cladding modes and analysed spectral features. When smaller *PM* values are used, the result may be subject to error, especially in the case of TFBGs having a slight tilt. This is due to the occurrence of a significant number of local minima

Table 3	Fanturas	extraction	rocult	for	DM = 200/2
Table 3.	reallires	extraction	resiiii	1Or	P/V = 30%

Θ	Correctly identified cladding mode minima	Additional minima detected	Not detected minima	Correctly identified cladding mode range
1	100.0%	0.0%	3.7%	yes
2	100.0%	0.0%	0.0%	yes
3	100.0%	0.0%	0.0%	yes
4	100.0%	0.0%	0.0%	yes
5	100.0%	0.0%	0.0%	yes
6	100.0%	0.0%	0.0%	yes
7	100.0%	0.0%	0.0%	yes
8	100.0%	0.0%	0.0%	yes
9	100.0%	0.0%	0.0%	yes
10	100.0%	0.0%	0.0%	yes

in the spectrum resulting from signal noise. The height of these minima may exceed 10% of the height of the biggest minimum of the cladding modes. Decreasing the value of the PM parameter results in an attempt to detect cladding modes having insignificant heights. If these heights are close to the height of the minima resulting from spectrum noise, it will be impossible to determine the limit of the cladding mode range. It will also be impossible to filter out undesired minima detected in the cladding mode range. This problem is illustrated in Figure 11, where the results obtained for TFBG with  $\Theta = 1$  and PM = 10% are shown. At wavelengths 1546.5 nm and 1547 nm, additional minima, positioned between cladding mode minima, were detected. They have not been filtered out due to insufficient height difference between them and the neighbouring cladding mode minima. On the spectrum shown in Figure 11 at wavelength 1560.3, a minimum is visible that was not identified because it was too close to another, higher minimum.

Figures 11 and 12 show the results of the algorithm implementing the developed method for different spectra. As shown in Figure 11, the spectrum of  $\Theta=1^\circ$  TFBG exhibits a Bragg resonance much larger than the minima of cladding modes, whereas in the case of  $\Theta=5^\circ$ , as presented in Figure 12, this proportion is reversed. The range of the identified cladding modes is marked red. In both presented cases, the cladding mode region and the Bragg resonance were identified correctly.

#### **Identifying the Bragg resonance**

Bragg resonance is searched for in the wavelength range longer than the maximum wavelength of the cladding modes. In the process of identifying the cladding mode range, a value of PM=20% was experimentally selected. This value enables the reliable determination of the accepted limit of the cladding mode range. At the same time, it allows for optimising the search

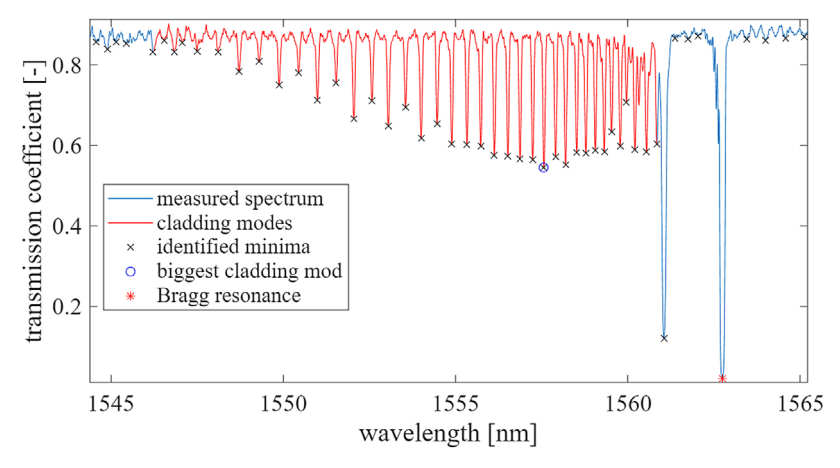


**Figure 11.** Spectrum features extraction for  $\Theta$ =1° and PM=10%

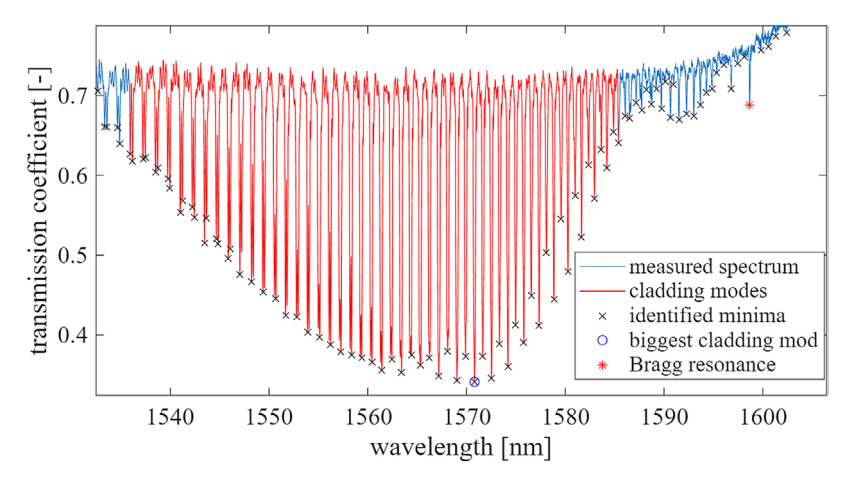


**Figure 12.** Spectrum features extraction for  $\Theta$ =5° and PM=20%

process. Most of the minima with significant height will be included in the cladding mode range. It automatically eliminates them from further analysis in the Bragg minimum identification process, reducing the computational cost. Since the Bragg minimum is identified based on the analysis of neighbouring minima height differences, its detection with the proposed method is possible only when it is at least twice the median height of neighbouring minima. The performed tests showed that the proposed algorithm correctly detects the Bragg minimum for TFBGs having  $\Theta \le 6^{\circ}$ . For TFBGs with larger angles, the algorithm returned information that detecting the Bragg mode was impossible. The study did not identify a case of incorrect detection of Bragg resonance.

#### Algorithm performance

One of the key aspects of any algorithm is its computational complexity and execution time [36]. The execution time of the presented algorithm was verified by running a single-threaded instance in the Matlab 2025a environment on a computer equipped with an Intel Core<sup>TM</sup> i5-1345U processor clocked at 1.6 GHz. The time measurement was started after loading the data from the disk and ended when the program finished running. The timing was performed for transmission spectra obtained from TFBGs with tilt angles  $\Theta = \{1^{\circ}, 2^{\circ}, ..., 10^{\circ}\}$ . For each spectrum, the measurement was repeated ten times. The median execution time was 0.0361 seconds, with a standard deviation of 0.0068 seconds, indicating low variability in runtime. The minimum observed time was 0.0274 seconds, while the

maximum reached 0.0477 seconds. This level of consistency demonstrates the algorithm's stable computational performance across repeated runs.

The algorithm's execution time is low and can be reduced further by using a different programming language and implementing multithreading. This enables the proposed solution to be utilised in real-time systems.

### Polynomial degree adjustment

To minimise the impact of the light source on the TFBG transmission spectrum, the transmission spectrum was divided by an approximated light source spectrum. The reason for using approximation was the noise present in the light source spectrum. This approximation was performed using polynomial interpolation. However, selecting the appropriate polynomial degree was necessary. A degree that is too low would not accurately represent the spectrum, while a degree that is too high could lead to overfitting, increasing the noise in the approximated spectrum. To determine the optimal degree, 10 recorded spectra of light reaching the TFBG were chosen. Each spectrum was approximated using polynomials of degree three to ten. Subsequently, the MAE between the spectra and their approximations was calculated. The average MAE values for various polynomial degrees are presented in Table 4. Figure 13 depicts the approximation graphs of an example light spectrum with polynomials of different degrees. The results indicated that polynomials up to the seventh degree could not accurately model the light source spectrum. An eighth-degree polynomial, however, provided a correct approximation, although it introduced

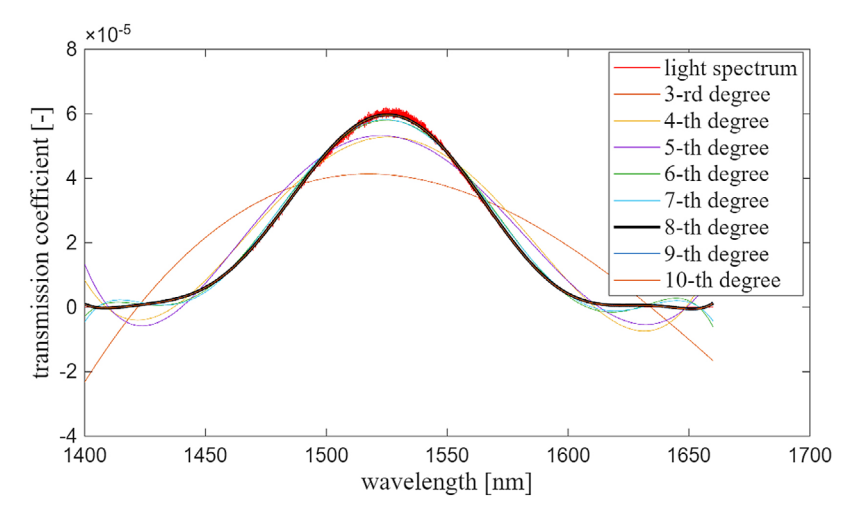


Figure 13. Light source spectrum approximation using different degree polynomials

**Table 4.** MAE of light source spectrum approximation using different degree polynomials

0 0 1 7		
Polynomial degree	MAE	
3	1.39 × 10 <sup>-10</sup>	
4	2.54 × 10 <sup>-11</sup>	
5	2.3 × 10 <sup>-11</sup>	
6	2.36 × 10 <sup>-12</sup>	
7	2.1 × 10 <sup>-12</sup>	
8	2.38 × 10 <sup>-13</sup>	
9	2.38 × 10 <sup>-13</sup>	
10	2.36 × 10 <sup>-13</sup>	

distortions at the edges of the interval. Using polynomials above degree eight slightly reduced MAE, but mostly overfitted noise. Additionally, higher degrees increased computational complexity. Consequently, an eighth-degree polynomial was chosen for this study.

#### **CONCLUSIONS**

Extraction of spectral features is challenging due to the significant variation of TFBG spectra with different  $\Theta$  angles and their considerable noise. Attempts to reduce the level of noise by filtering the spectrum did not yield the expected result. It is due to the signal distortion introduced and the loss of some information relevant to the analysis. Developing a spectrum feature extraction method required the development of complex signal analysis algorithms.

The developed method for analysing TFBG spectrum features is pioneering work. It provides

a basis for further work leading to the automation of the process of selecting wavelength ranges or cladding mode minima for use in measurements performed using TFBGs.

The present method of extraction of selected features of the TFBG spectrum allows analysis of spectra measured for S and P polarisations. It successfully detects cladding mode minima in the range of 20–100% of the highest cladding mode minimum height. It allows for the identification of the wavelength range in which the cladding mode region is located, the calculation of the height of the individual minima, and the identification of the largest one. The method also detects the Bragg resonance if its height is more than twice the median of nearby minima.

The proposed algorithm is designed for feature extraction from light spectra obtained from straight TFBGs. Using the algorithm with TFBGs subjected to bending, twisting, or coating requires additional modifications.

The algorithm's limitations, discussed in the text, do not affect the correct identification of the analysed spectral features.

Future work: due to the high complexity of the minima detection algorithm, it should be interesting to investigate the possibility of detecting spectrum minima using machine learning techniques successfully used in other applications [37,38]. The other research field is to extend feature detection to spectra measured at any polarisation. It would also be interesting to examine the possibility of a spectrogram [39] and statistical dependencies [40] usage in future research.

#### **REFERENCES**

- Jean-Ruel H, Albert J. Recent advances and current trends in optical fiber biosensors based on tilted fiber bragg gratings. TrAC, Trends Anal Chem 2024;174:117663. https://doi.org/10.1016/j.trac.2024.117663
- Butov OV, Tomyshev KA, Nechepurenko IA, Dorofeenko A V, Nikitov SA. Tilted fiber Bragg gratings and their sensing applications. Phys -Usp 2022;65:1290–302. https://doi.org/10.3367/ UFNe.2021.09.039070
- 3. Klimek J. The impact of changes in the apodization profile of the Bragg grating on its spectral characteristics. Przegl El 2023;99:330–3. https://doi.org/10.15199/48.2023.01.68
- Wojcik J, Mergo P, Makara M, Poturaj K, Czyzewska L, Klimek J, et al. Technology of suspended core microstructured optical fibers for evanesced wave and plasmon resonance optical fiber sensors. In: Kalli K, Urbanczyk W, editors. PCF. II, 6990, 2008. https://doi.org/10.1117/12.783327
- 5. Skorupski K, Miluski P, Harasim D, Klimek J, Panas P, Kisała P. Effect of Tm3+ ion doping on the possibility of Bragg resonator inscription using an excimer laser. Metrol and Meas Syst 2024;31:595–608. https://doi.org/10.24425/mms.2024.150284
- 6. Shedreyeva I, Karnakova G, Sakhno O, Biezkrevnyy O, Uvaysova A, Karas O. The influence of the TFBG tilt angle on the spectral response. In: Romaniuk RS, Smolarz A, Wojcik W, editors. Photonics Applications in Astronomy, Communications, Industry, and High Energy Physics Experiments 2021, vol. 12040, 2021. https://doi.org/10.1117/12.2617727
- 7. Huang F, Moreno Y, Cai J, Cai L, Cai H, Dai Y, et al. Refractive index sensitivity characterization of tilted fiber Bragg grating based surface plasmon resonance sensor. J Lightwave Technol 2023;41:5737–43.
- Singh Y, Raghuwanshi SK, Prakash O, Saini PK. Design and development of tilted fiber Bragg grating (TFBG) chemical sensor with regression analysis of grating parameters for sensitivity optimization. Opti Quant Electron 2021;53. https://doi. org/10.1007/s11082-021-03328-6
- 9. Kisala P. Physical foundations determining spectral characteristics measured in Bragg gratings subjected to bending. Metrol and Meas Syst 2022;29:573–84. https://doi.org/10.24425/mms.2022.142275
- Harasim D, Cięszczyk S. A novel method of elimination of light polarization cross sensitivity on tilted fiber Bragg grating bending sensor. Metrol and Meas Syst 2022;29:737–49. https://doi.org/10.24425/mms.2022.143066
- 11. Koziel G, Harasim D, Dziuba-Koziel M, Kisala P.

- Fourier transform usage to analyse data of polarisation plane rotation measurement with a TFBG sensor. Metrol and Meas Syst 2024;31:369–81. https://doi.org/10.24425/mms.2024.149698
- 12. Dziuba-Koziel M, Koziel G, Harasim D, Kisala P, Kochanowicz M. Method of automatic calibration and measurement of the light polarisation plane rotation with tilted fibre Bragg gratings and discrete wavelet transform usage. Adv Scie Tech Res J 2025;19:165–77. https://doi.org/10.12913/22998624/194890
- 13. Liu Y, Li Y, Xu P, Yu C. Temperature and lateral pressure sensing using a sagnac sensor based on cascaded tilted grating and polarization-maintaining fibers. Sens 2024;24. https://doi.org/10.3390/s24216779
- 14. Li P, Huang Y, Wang E, Cao J, Pei Y, Lyu G. Tilted fiber Bragg grating pH sensor based on polyaniline reaction deposition film layer. Opti Quant Electron 2024;56. https://doi.org/10.1007/s11082-024-07268-9
- 15. Wen H-Y, Lee K-M, Chen R-Y, Chen S-Y, Chiang C-C. Capture and sensing of mercury ions by self-assembly supramolecular carbene complexes on tilted fiber Bragg grating (TFBG) sensors. Meas 2024;236. https://doi.org/10.1016/j.measurement.2024.115152
- 16. Harasim D. Polarization-insensitive Refractive Index Measurement Using Cascaded Perpendicular Tilted Fiber Bragg Gratings. Meas 2022;202:111845. https://doi.org/https://doi.org/10.1016/j.measurement.2022.111845
- 17. Zhu T, Chah K, Loyez M, Caucheteur C. Partially-coated TFBGs for biosensing. In: Berghmans F, Zergioti I, editors. Optical Sensing and Detection 2022;VII:12139. https://doi.org/10.1117/12.2625408
- 18. Ribaut C, Loyez M, Larrieu J-C, Chevineau S, Lambert P, Remmelink M, et al. Cancer biomarker sensing using packaged plasmonic optical fiber gratings: Towards in vivo diagnosis. Biosens Bioelectron 2017;92:449–56. https://doi.org/https://doi. org/10.1016/j.bios.2016.10.081
- 19. Yuan Y, Guo T, Qiu X, Tang J, Huang Y, Zhuang L, et al. electrochemical surface plasmon resonance fiber-optic sensor: in situ detection of electroactive biofilms. Anal Chem 2016;88:7609–16. https://doi.org/10.1021/acs.analchem.6b01314
- Avellar L, Marques CAF, Caucheteur C, Frizera A, Leal-Junior A. Comprehensive evaluation of tilted fiber Bragg grating (TFBG) sensors for characterizing oilwater emulsions: a study on the impact of surfactant concentration and mixing speed. IEEE Sens J 2024;24:7824–31. https://doi.org/10.1109/ JSEN.2024.3354947
- 21. Zheng H, Liu Z, Li S, Feng D, Jiang B. Pd/WO3 co-deposited tilted fiber Bragg grating for fast hydrogen

- sensing. IEEE Trans Instrum Meas 2025;74. https://doi.org/10.1109/TIM.2024.3522415
- 22. Ren Z, Huang Z, Wang F, Wu J, Zhou J, Wang Z, et al. Tilted fiber Bragg grating surface plasmon resonance based optical fiber cadmium ion trace detection. Sens Actuators B: Chem 2023;393. https://doi.org/10.1016/j.snb.2023.134247
- 23. Zhang C, Chen X, Liu X, Shen C, Huang Z, Wang Z, et al. High sensitivity hydrogen sensor based on tilted fiber Bragg grating coated with PDMS/WO3 film. Int J Hydrogen Energy 2022;47:6415–20. https://doi.org/10.1016/j.ijhydene.2021.11.238
- 24. Chubchev E, Tomyshev K, Nechepurenko I, Dorofeenko A, Butov O. Machine learning approach to data processing of TFBG-assisted SPR sensors. J Lightwave Technol 2022;40:3046–54. https://doi.org/10.1109/JLT.2022.3148533
- 25. Li X, Zhang Q, Li J. Sensing performance comparison for temperature and liquid level sensor based on uniform and step-Etched microfiber TFBG. Infrared Phys 2024;142:105554. https://doi.org/10.1016/j.infrared.2024.105554
- 26. Fazzi L, Valvano S, Alaimo A, Groves RM. A simultaneous dual-parameter optical fibre single sensor embedded in a glass fibre/epoxy composite. Compos Struct 2021;270. https://doi.org/10.1016/j.compstruct.2021.114087
- 27. An G, Liu L, Hu P, Jia P, Zhu F, Zhang Y, et al. Probe type TFBG-excited SPR fiber sensor for simultaneous measurement of multiple ocean parameters assisted by CFBG. Opt Express 2023;31:4229–37. https://doi.org/10.1364/OE.481948
- 28. Powroznik P, Czerwinski D. Spectral Methods in Polish emotional speech recognition. Adv Scie Tech Res J 2016;10:73–81. https://doi.org/10.12913/22998624/65138
- 29. Korga S, Żyła K, Józwik J, Pytka J, Cybul K. Predictive tools as part of decission aiding processes at the airport the case of Facebook prophet library. Appl Comput Sci 2023;19:51–67. https://doi.org/10.35784/acs-2023-35
- 30. Lukaszuk T, Krawczuk J, Zyla K, Kesik J. Stability of feature selection in multi-omics data analysis. Applied Sciences-Basel 2024;14. https://doi.org/10.3390/app142311103
- 31. Manuylovich E, Tomyshev K, Butov O V. Method for determining the plasmon resonance wavelength in fiber sensors based on tilted fiber Bragg gratings.

- Sens 2019;19. https://doi.org/10.3390/s19194245
- 32. Tomyshev KA, Manuilovich ES, Tazhetdinova DK, Dolzhenko EI, Butov O V. High-precision data analysis for TFBG-assisted refractometer. Sens Actuators A: Phys 2020;308:112016. https://doi.org/https://doi.org/10.1016/j.sna.2020.112016
- 33. Cięszczyk S. Application of Gabor, log-Gabor, and adaptive Gabor filters in determining the cut-off wavelength shift of TFBG sensors. Appl Sci 2024;14. https://doi.org/10.3390/app14156394
- 34. Cięszczyk S, Harasim D, Skorupski K, Panas P, Klimek J. Influence of polarization on demodulation methods for determining the SRI value for a single TFBG and an orthogonal grating system. Opt Express 2024;32:43264–76. https://doi.org/10.1364/OE.540761
- 35. Kisała P, Kalizhanova A, Kozbakova A, Yeraliyeva B. Identification of cladding modes in SMF-28 fibers with TFBG structures. Metrol and Meas Syst 2023;30:507–18. https://doi.org/10.24425/mms.2023.146418
- 36. Tuiri SE, Sabil N, Benamar N, Kerrache CA, Koziel G. An EEG Based Key Generation Cryptosystem using Diffie-Hellman And AES. 2019 2nd IEEE Middle East and North Africa Communications Conference (IEEEMENACOMM'19), 2019;54–9. https://doi.org/10.1109/menacomm46666.2019.8988578
- 37. Powroźnik P, Skublewska-Paszkowska M, Nowomiejska K, Aristidou A, Panayides A, Rejdak R. Deep convolutional generative adversarial networks in retinitis pigmentosa disease images augmentation and detection. Adv Scie Tech Res J 2025;19:321–40. https://doi.org/10.12913/22998624/196179
- 38. Skublewska-Paszkowska M, Powroźnik P, Barszcz M, Dziedzic K, Aristodou A. Identifying and animating movement of Zeibekiko sequences by spatial temporal graph convolutional network with multi attention modules. Adv Scie Tech Res J 2024;18:217–27. https://doi.org/10.12913/22998624/193180
- Chwaleba K, Wach W. Polish dance music classification based on mel spectrogram decomposition. Adv Scie Tech Res J 2025;19. https://doi.org/10.12913/22998624/195506
- 40. Kowal B, Strzalka D. Statistical long-range dependencies and statistical self-similarity in computer systems processing the case of cache bytes counter. Adv Scie Tech Res J 2024;18:311–8. https://doi.org/10.12913/22998624/194428